Mutation-induced protein interaction kinetics changes affect apoptotic network dynamic properties and facilitate oncogenesis

Linjie Zhao[a], Tanlin Sun[b], Jianfeng Pei[b,1], and Qi Ouyang[a,b,c,1]

[a]State Key Laboratory for Artificial Microstructures and Mesoscopic Physics, School of Physics, Peking University, Beijing 100871, China; [b]Center for Quantitative Biology, Academy for Advanced Interdisciplinary Studies, Peking University, Beijing 100871, China; and [c]Peking-Tsinghua Center for Life Sciences, Academy for Advanced Interdisciplinary Studies, Peking University, Beijing 100871, China

Edited by José N. Onuchic, Rice University, Houston, TX, and approved June 17, 2015 (received for review February 4, 2015)

It has been a consensus in cancer research that cancer is a disease caused primarily by genomic alterations, especially somatic mutations. However, the mechanism of mutation-induced oncogenesis is not fully understood. Here, we used the mitochondrial apoptotic pathway as a case study and performed a systematic analysis of integrating pathway dynamics with protein interaction kinetics to quantitatively investigate the causal molecular mechanism of mutation-induced oncogenesis. A mathematical model of the regulatory network was constructed to establish the functional role of dynamic bifurcation in the apoptotic process. The oncogenic mutation enrichment of each of the protein functional domains involved was found strongly correlated with the parameter sensitivity of the bifurcation point. We further dissected the causal mechanism underlying this correlation by evaluating the mutational influence on protein interaction kinetics using molecular dynamics simulation. We analyzed 29 matched mutant–wild-type and 16 matched SNP—wild-type protein systems. We found that the binding kinetics changes reflected by the changes of free energy changes induced by protein interaction mutations, which induce variations in the sensitive parameters of the bifurcation point, were a major cause of apoptosis pathway dysfunction, and mutations involved in sensitive interaction domains show high oncogenic potential. Our analysis provided a molecular basis for connecting protein mutations, protein interaction kinetics, network dynamics properties, and physiological function of a regulatory network. These insights provide a framework for coupling mutation genotype to tumorigenesis phenotype and help elucidate the logic of cancer initiation.

mutation-induced oncogenesis | dynamic bifurcation | parameter sensitivity analysis | mutation enrichment | protein interaction kinetics

High-throughput whole-genome sequencing (1) and massively parallel technologies (2) have enabled cancer researchers to understand that cancer is a disease caused primarily by genomic alterations, especially somatic cell mutations (3, 4). This stimulated extensive research endeavors to identify the landscape of cancer-related mutations. In the last decade, studies of different tumor types using cancer genomic and pathology analysis indicate that oncogenic mutations are concentrated primarily in a few core regulatory pathways that govern cell phenotypic behaviors (5–8). These results led to the idea that "genetic aberrations alter normal cellular regulation and then drive tumor development" (9, 10). Therefore, mutation-induced oncogenesis should be explored from a network and system perspective.

A systematic interpretation of oncogenesis can be achieved in part by analyzing interactions among mutated genes and performing functional annotation of cancer-related proteins in functional pathways. A more quantitative approach is network modeling using ordinary differential equations (ODEs) and mathematical simulations. This well-established method has been successfully used to understand cellular dynamic functionalities and network regulatory principles, including the relationship between genetic mutations and oncogenesis (11–15). For example, Stites et al. (14) studied common oncogenic Ras mutations that affect Ras activation. They performed ODE model simulation to investigate the steady-state Ras concentration response to kinetic parameter changes and found a strong correlation between oncogenic mutations and Ras activation level. Chen et al. (15) recently analyzed the p53-induced apoptosis model and found that parameters significantly affecting the system's bifurcation points corresponded with frequently mutated oncogenic genes. These studies demonstrate the suitability of applying systems-level analysis to understand oncogenesis. However, the limitations of previous analyses are obvious. Only pure network-based dynamics analyses were conducted, in which proteins were abstracted as theoretical nodes, structural details of interactions were ignored, functional processes of protein conformational changes were oversimplified, only correlations between mutations and dynamic properties were analyzed, and the causal molecular clues for the oncogenic function of cancer-related mutations remained unexplored.

In this study, we investigate the causal mechanisms of mutation-induced oncogenesis by integrating network-based dynamics modeling with structural-based mutation analysis and molecular dynamics simulation of protein interactions. This approach enables us to map cancer-related mutations to network dynamics changes via protein–protein interaction kinetics. We propose that cancer-related gene mutations may change relevant protein interaction kinetics in the network, which directly change the network's model parameters. Subsequently, some of these disturbances may qualitatively change system dynamics behaviors, thereby disrupting normal cellular processes, and ultimately causing cancer.

Significance

Cancer is highly correlated with somatic mutations. Understanding how mutation induces oncogenesis is an important task in cancer research. We proposed a strategy that combined network-based dynamics modeling with structural-based mutation analysis and molecular dynamics simulation to map cancer-related mutations to network dynamics changes via protein–protein interaction kinetics. This approach identifies the oncogenic role of mutations and subsequently determines the causal mechanism of mutation-induced oncogenesis. This work provides a framework for coupling mutation genotype to tumorigenesis phenotype. It is also a step toward seeking more effective anticancer drug targets in cellular pathways.

Author contributions: L.Z., T.S., J.P., and Q.O. designed research; L.Z. and T.S. performed research; L.Z. and T.S. analyzed data; and L.Z., T.S., J.P., and Q.O. wrote the paper.

The authors declare no conflict of interest.

This article is a PNAS Direct Submission.

Freely available online through the PNAS open access option.

[1]To whom correspondence may be addressed. Email: jfpei@pku.edu.cn or qi@pku.edu.cn.

This article contains supporting information online at www.pnas.org/lookup/suppl/doi:10.1073/pnas.1502126112/-/DCSupplemental.

We used the mitochondrial apoptotic pathway as a case study to validate our hypothesis, because dysfunction of this pathway may lead to many diseases, including cancer (16). After we constructed a mathematical model for the regulatory network based on mass action kinetics, we established the functional role of dynamic bifurcation in apoptosis and used parameter sensitivity analysis to examine the nonuniform effect of parameter variation on the bifurcation point using techniques developed during our previous work (15). We also investigated oncogenic mutations involved in the network by mapping them onto 3D protein structures and identified mutation enrichment for each protein functional domain. We found that cancer-related mutations also have a nonuniform distribution among different functional domains, and this distribution is strongly correlated with the nonuniformity of parameter sensitivity of the bifurcation point. We further dissected the causal mechanism underlying this correlation by evaluating mutational influence on protein interaction kinetics using molecular dynamics simulation. We found that the mutation-induced binding energy change is a major cause of parameter changes in the regulatory network model, and the kinetics changes of protein interactions that induce variations in the bifurcation point sensitive parameters are a major cause of apoptosis pathway dysfunction. We identified the oncogenic role of each mutation by combining the bifurcation point change direction due to parameter perturbation and the binding energy change direction due to mutation disturbance and found that mutations involved in sensitive interactions (corresponding to sensitive parameters of the bifurcation point) are most likely oncogenic.

Our approach, which couples pathway dynamics with protein interaction kinetics, provides a molecular basis for connections among protein mutations, protein interaction kinetics, network dynamics properties, and physiological function of a regulatory network. This work bridges the gap between genotype (mutations) and phenotype (tumorigenesis) and validates the hypothesis that mutation-induced abnormal changes in biological system dynamic properties may be a major cause of cancer initiation and development.

Results

Model Construction and Nonlinear Dynamics Analysis. Apoptosis is a highly regulated process that is strongly dependent on mitochondrial function (16). We constructed a simplified apoptotic network focused primarily on the regulation of mitochondrial outer membrane permeabilization (MOMP), where cross-talk between intrinsic and extrinsic pathways occurs and multiple apoptotic signals culminate (17). MOMP is a primary cause of cell apoptosis; it leads to irreversible cell death by releasing proapoptotic factors such as cytochrome *c* and Smac from the mitochondrial intermembrane space and subsequently facilitating caspase activation (18). MOMP is controlled primarily through interactions among Bcl-2 protein family (19). Bcl-2 family members can be classified into two groups: pro- and antiapoptotic factors. The former contains the following three subtypes: the MOMP effectors Bax and Bak; Bax and Bak activators such as Bid and Bim; and sensitizers such as Puma and Noxa. Antiapoptotic members such as Bcl-2, Bcl-xL, and A1 can be considered as inhibitors of Bax and Bak association (20).

We performed extensive data survey and collection and constructed the MOMP core regulatory network triggered by extrinsic stimulus (Fig. 1). During apoptosis, initiator caspases such as caspase8 that have been activated by the death-inducing signaling complex (DISC; not shown in our network) cleave Bid into the active form tBid (21). Then, tBid promotes a series of conformational changes in Bax, resulting in its translocation from the cytosol onto the mitochondrial outer membrane (MOM) (22). Active Bax monomers incrementally form oligomers and create pores in MOM, consequently causing MOMP (23). The antiapoptotic proteins A1 and Bcl-2 bind tBid and Bax in the cytoplasm and on the membrane to inhibit effector activation (24), whereas the membrane-bound Bax dimer undergoes autoactivation to generate a positive feedback loop that enhances oligomer accumulation (25). Puma binds to both A1 and Bcl-2 to neutralize the inhibitors and release the effectors from the protein complex, and Noxa specifically binds to A1 (26).

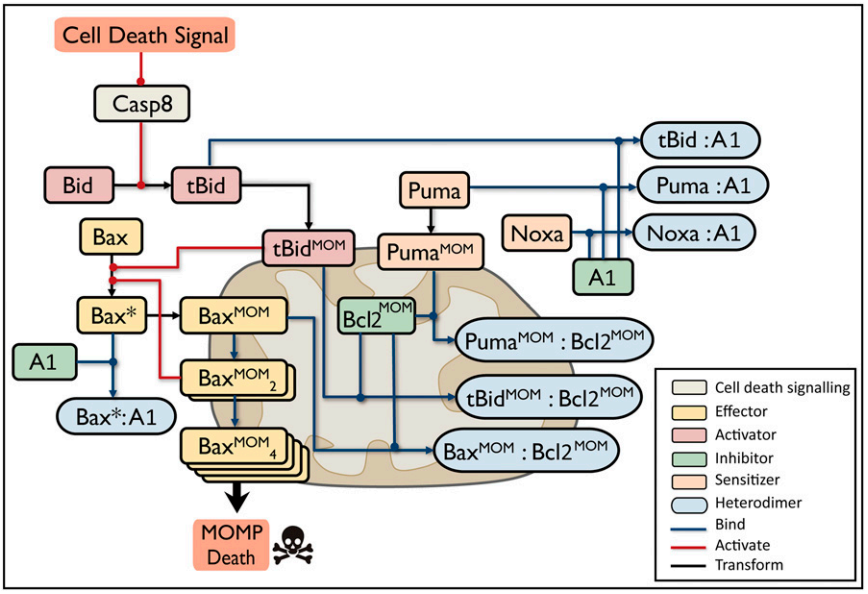

Fig. 1. Extrinsic signal-induced mitochondrial apoptotic pathway. Blue lines indicate binding, red lines indicate activation, and black lines indicate conformational transformation. Bax*, activated Bax; colon, protein complex; MOM superscript, proteins on mitochondrial outer membrane. Different functions of Bcl2 family proteins, such as Activator, Inhibitor, Effector, and Sensitizer, are colored in red, green, yellow, and orange, respectively. Heterodimers are colored in blue. Apoptosis is induced by activated caspase8; Bax oligomers (denoted by Bax^{MOM}_4) create pores in the mitochondrial outer membrane, which causes MOMP and cell death initiation. Proteins with redundant function are compressed into a representative reactant; Bax and Bak are represented by Bax, and Bcl2, Bcl-xl, and Mcl-1 are represented by Bcl2.

Fig. 1 is a simplified network with compressions of redundancy (see *Supporting Information* for details). Compared with previous apoptotic models (15, 27), our model distinguishes the cytoplasmic and membrane binding of antiapoptotic proteins and elaborates the conformational changes and translocation processes of proapoptotic proteins. These processes are essential for triggering MOMP (28) and understanding mitochondrial apoptosis.

We used well-established methods for describing signaling pathways (29) and built a set of ODEs according to Fig. 1 to simulate the MOMP apoptotic network. The model parameters were chosen based on experimental data and reasonable estimates of biochemical constraints (Table S1). We conducted nonlinear dynamics analysis to study the system dynamics behavior. The model input and output was the caspase8 concentration and the Bax oligomer concentration, respectively. The analysis identified a saddle-node bifurcation of Bax oligomer concentration as a function of caspase8 concentration (Fig. 2, black line). There is a bistable regime in which two stable steady states of Bax oligomer concentration coexist (Fig. 2). The low and high branches in the bistable regime indicate that the apoptosis pathway is in the OFF and ON states, respectively. With increasing caspase8 levels, the system changes from a bistable state to a monostable state via the saddle-node bifurcation. When the system is in the OFF state, a sudden increase in Bax oligomer concentration will occur if the active caspase8 concentration increases beyond the bifurcation point. This kind of transition can be regarded as a life-to-death switch of a cell under apoptotic stimulus. Therefore, the location of the bifurcation point (i.e., critical concentration of caspase8) reflects the death threshold.

Parameter Sensitivities. Previous studies established that dynamic bifurcations manifest qualitative changes in biological systems and govern many biological functions (15, 30, 31). In our system, the saddle-node bifurcation provides the mechanism of the life-to-death switch. The location of the bifurcation point determines when a cell undergoes apoptosis; therefore, it determines the cell's fate. Changes in certain parameters may lead to a large change at the location of the critical point, which can render the system dysfunctional. An example of such an effect in the MOMP network is presented in Fig. 2. Our simulation shows that a 30% reduction in the tBid–Bcl2 dissociation rate in the regulatory network significantly shifts the bifurcation point to the right from the original wild-type location, so that a much stronger caspase8 signal is required to switch on apoptosis. When this parameter is reduced by 70% or more, high levels of Bax oligomer can never be reached even under extremely strong apoptotic stimulus, so cell apoptosis is completely shut off. These cellular conditions provide a possible background for oncogenesis.

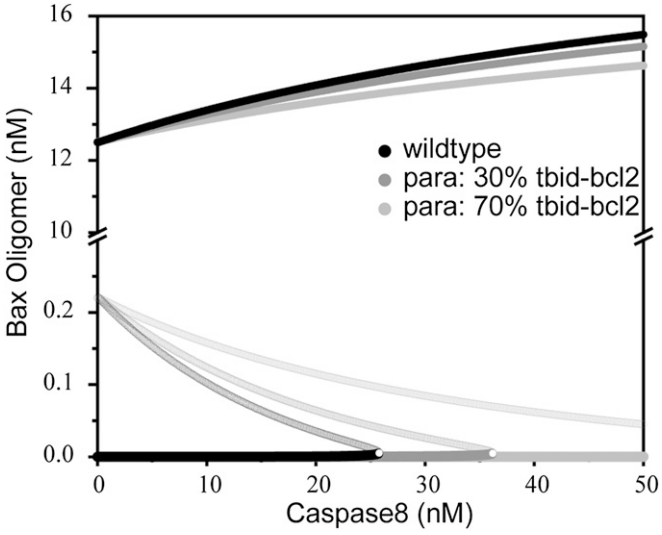

Fig. 2. Bifurcation diagram for Bax oligomer in MOMP induction. Bifurcation diagram for Bax oligomers using the caspase8 concentration as the control parameter. Solid circles indicate the stable steady state; open circles indicate the unstable state. Reducing the parameter tBid-Bcl2 shifts the bifurcation point to the right, indicating an increasing MOMP threshold. Black, without tBid-Bcl2 decrease; dark gray, tBid-Bcl2 decreased by 30%; light gray, tBid-bcl2 decreased by 70%.

The nonuniform effect of parameter variation on dynamic properties has been reported in many biological systems (15, 32, 33). In our model, the effect of parameter changes on the bifurcation point location is not evenly distributed. To identify which parameters have a major impact on the bifurcation point location in our model, we conducted single-parameter sensitivity analysis to the bifurcation point by increasing or decreasing each of the 52 model parameters by 10% and recorded the percentage change of the bifurcation point. A sensitivity spectrum of all parameters was achieved in this way (Fig. 3*A*). Using the method of *k*-means clustering, we separated the parameters into the following four clusters according to their impact on the bifurcation point location: most sensitive, sensitive, insensitive, and most insensitive. A more systematic analysis of the model parameter sensitivity (change each parameter by 1%, 5%, 10%, and 15%) shows that the sensitivity patterns are approximately the same among the spectrums obtained through different parameter perturbation degree. Clustering analysis on each spectrum also shows the same cluster cutoff location between different sensitivity clusters (Fig. S1 *A* and *B*). A right shift of the bifurcation point suggests an increasing oncogenic potential. Therefore, the direction of parameter perturbation (increasing or decreasing) that leads to a right shift of the critical point is chosen (see the blue and orange bars in Fig. 3*A*). The direction change resulting from parameters in the most insensitive class is not discriminated, because their influences on the bifurcation point location can be neglected.

To map cancer-related mutations to network dynamic changes via protein interaction kinetics, we narrowed our study to the parameters of protein interactions in which the effect of genetic variation is due primarily to mutations in the corresponding functional domains. We selected a subset of the sensitivity spectrum from the parameter sensitivity spectrum of Fig. 3*A* in which only the parameters that represent specific protein interactions were chosen (Fig. 4*A*, *Left*). The subset includes the parameters of protein–protein binding and activation rate (Fig. 3*B*) and the parameters of membrane localization rate (Fig. 3*C*) but excludes the parameters of protein production and degradation rates (Fig. 3*D*). The latter can be affected by many mechanisms, such as mutations in promoter regions, transcription factors, chromosome translocation, and proteasome; these parameters cannot be explained simply by the kinetics of protein interactions. This selection allowed us to evaluate mutational influence on protein interaction kinetics using mutation domain mapping and molecular dynamics simulation, through which the parameter sensitivity of the bifurcation point and cancer-related mutations can be linked on a molecular basis.

Cancer-Related Mutation Enrichment. To characterize the mutation pattern in our model and its association with the parameter sensitivity spectrum, we manually collected cancer-related mutations from the Catalogue of Somatic Mutations in Cancers (COSMIC) database (34) and from the literature (35). We focused primarily on missense mutations and ignored all SNPs nominated in the dbSNP database (36) (Table S2). Our analysis is different from previous studies that simply counted the total mutation number for each protein (15). For a given protein interaction (corresponding to the parameters in Fig. 4*A*, *Left*), we first distinguished functional and nonfunctional domains for involved proteins

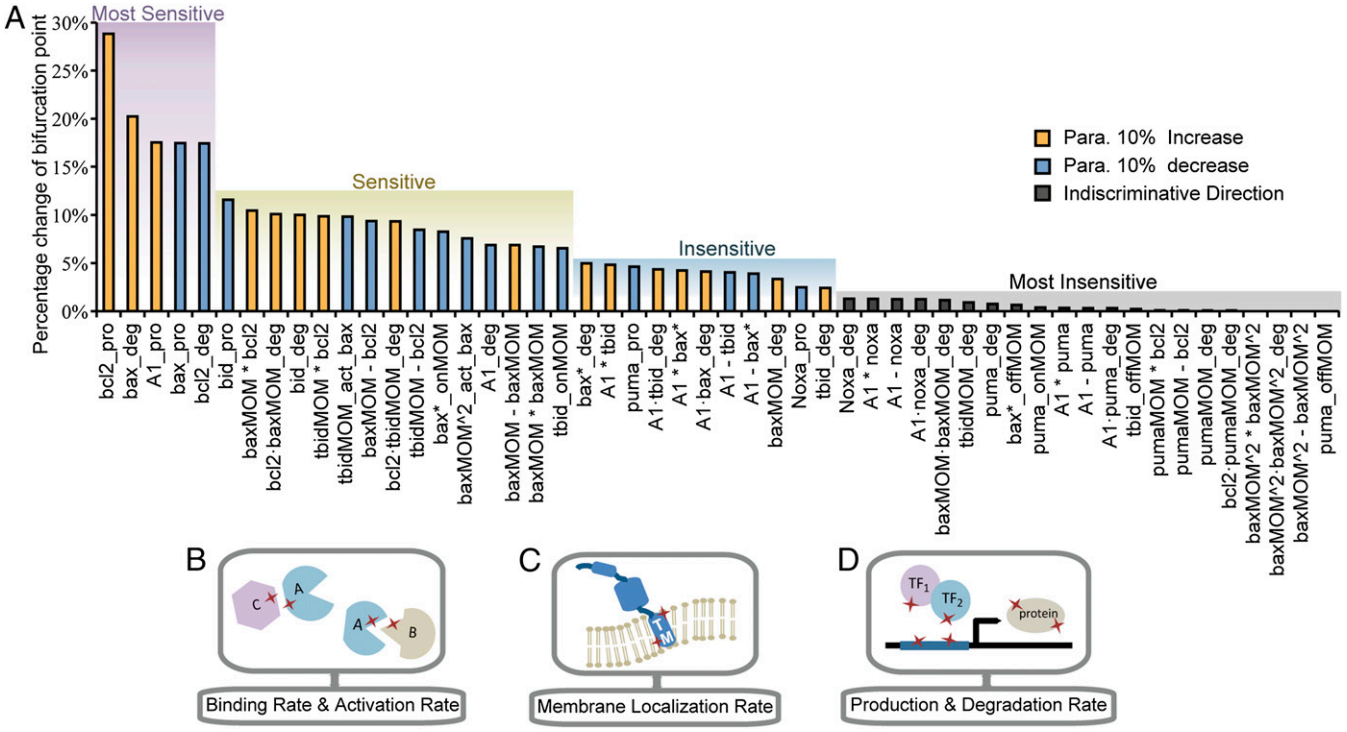

Fig. 3. Parameter sensitivity spectrum and parameter types. (*A*) Percentage change of the bifurcation point in response to 10% increase or decrease of each parameter. Color bars indicate the perturbation direction of each parameter. Horizontal coordinates indicate the corresponding interactions for each parameter. See Table S1 for details of the correspondence between parameters and represented interactions. asterisk, association; deg, degradation rate; onMOM/offMOM, membrane translocation and membrane separation; pro, production rate; minus, dissociation. (*B*) Illustration of mutation location influencing protein–protein interactions such as binding or activating. (*C*) Illustration of mutation location influencing translocation rate of proteins to the membrane. TM, transmembrane domain. (*D*) Illustration of mutation locations influencing protein production and degradation rates. Red stars indicate the mutation location.

according to their structural information and then mapped all mutations to the functional and nonfunctional domains. Details regarding the basis and definition of functional and nonfunctional domains are given in *Supporting Information* and Table S3.

To quantify the cancer mutation distribution, we calculated the mutation enrichment for each of the functional domains (Table S4). Mutation enrichment for a functional domain is defined as $E_i = (M_i/M_i + M_{non\_fun})/(L_i/L_i + L_{non\_fun})$, where M_i and L_i denote, respectively, the number of mutations and the amino acid length in the functional domain i; M_{non_fun} and L_{non_fun} denote, respectively, the number of mutations and the amino acid length in nonfunctional domains of the corresponding proteins. This definition of mutation enrichment tends to normalize different functional domain mutations in different proteins.

The spectrum of the enrichment value is listed in Fig. 4*A*, *Right*. For each protein interaction (e.g., interaction of protein A and B), the enrichment value for a domain in protein A and a domain in protein B is evaluated separately. We also calculated the combined enrichment of protein A and protein B to characterize the whole interaction (see the definition of the combined enrichment in *Supporting Information*). Naturally, $E = 1$ can be considered as a separation of low- and high-density oncogenic mutations in a given protein interaction domain of a given protein; a domain with $E > 1$ indicates that more oncogenic mutations are concentrated in this protein interaction domain than in nonfunctional domains of the given protein. This domain mapping more accurately reflects the correspondence between cancer mutations and model parameters.

Comparison Between Parameter Sensitivity and Mutation Enrichment. The sensitivity spectrum of the subset parameters can be clearly grouped into three parameter clusters: sensitive, insensitive, and most insensitive (Fig. 4*A*, *Left*). Each cluster covers distinct features. Most parameters in the first cluster (sensitive) correspond to interactions of apoptotic regulators on MOM, such as Bcl2, Bax^{MOM} and $tBid^{MOM}$, which are indispensable and dominant processes in the network. The parameters depicting the interactions, in which cytosolic reactants and some BH3 proteins with redundant functions participate, belong to the last two clusters (insensitive and most insensitive). Comparing Fig. 4*A*, *Left* and *Right*, we found good correlation between the parameter sensitivity of the bifurcation point and the mutation enrichment of each corresponding functional domain. Specifically, most of the sensitive parameters correspond to functional domains with high mutation enrichment, whereas the domains corresponding to insensitive parameters have relatively low mutation enrichment. A clear correlation between parameter sensitivity and combined mutation enrichment is shown in Fig. 4*B*. With increasing value of parameter sensitivity, the corresponding combined mutation enrichment generally tends to increase, which indicates that sensitive interactions tend to carry relatively greater numbers of mutations.

This correlation pattern is in agreement with most experimental results reported in the literature. For example, mitochondrial localization and insertion of Bax with its C-terminal transmembrane (TM) region (168–193 aa) (the corresponding parameter in our model is Bax*_onMOM) is a necessary step for MOMP and apoptotic induction (37). Schinzel et al. (38) proved that removal of Bax C-terminal or substitution of residue 168 in HeLa cells attenuated Bax localization at the mitochondria and apoptotic function. Gil et al. (39) reported that mutation of Bax residue 169, which was identified as a mutation hot spot in gastrointestinal cancer by Yamamoto et al. (35), reduced cell death by disrupting Bax membrane location. The loss-of-function mutations in Bax C-terminal TM region reduce the translocation

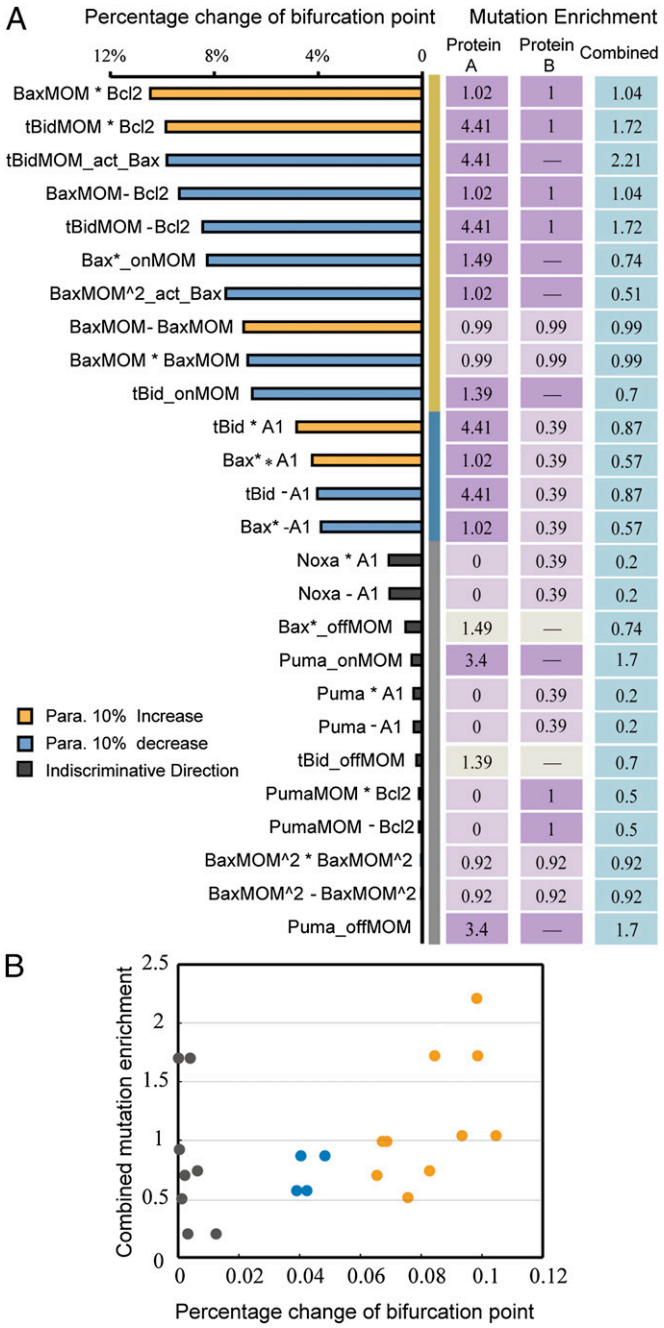

Fig. 4. Comparison between subset parameter sensitivities and mutation enrichment for each functional domain. (*A*) Comparison between subset parameter sensitivities and mutation enrichment. Different sensitivity groups are separated by yellow, blue, and gray stripes, with the same criteria as those of Fig. 3*A*. Bar colors indicate perturbation direction for each parameter. Corresponding interactions for each parameter are labeled. Cancer-related mutation enrichment for each corresponding functional domain is aligned to the corresponding parameters. Protein A, first protein in the interaction; Protein B, second protein in the interaction; Combined, combined mutation enrichment for corresponding interation. Enrichments for interactions only involving one protein are marked by a dash in the Protein B panel. Dark purple, $E \geq 1$; light purple, $E < 1$; ivory, inconsistent sensitivity between the membrane translocation parameter and the membrane separation parameter. (*B*) Two-dimensional scatter plot of subset parameter sensitivity and combined mutation enrichment. Dot colors indicate different sensitivity groups.

rate of activated Bax. Our sensitivity analysis showed that Bax*_onMOM is indeed a sensitive parameter; a slight decrease in Bax*_onMOM shifts the bifurcation point to the right. Consistent with the result identifying Bax as a sensitive parameter, relatively high mutation enrichment was identified in the Bax C-terminal TM domain. Nevertheless, we found some exceptions. Sensitivity analysis showed that the parameters describing Puma membrane translocation are really insensitive, whereas the mutation enrichment of the corresponding domain (Puma_onMOM: 1.7) is much greater than that for Bax (Bax homodimerization, 0.99), whose dimerization is identified as a sensitive interaction. This might result from the complexity of Bax–Bax interactions. On one hand, multiconformational changes during Bax functioning may bring uncertainty and overlap into functional domains of homodimerization and oligomerization, which made it difficult to map mutations clearly. However, for Puma membrane translocation, the functional domain (C-terminal transmembrane domain) is more independent and clear. On the other hand, Bax has different protein moieties that participate in many more interactions than other apoptotic regulators, so the nonfunctional domain is much shorter. This may help to understand why mutation enrichments for Bax-involved interactions are approximately the same and close to 1 (Bax homodimerization, 0.99; Bax oligomerization, 0.92).

The results presented in Fig. 4 support the previous observation (15) that the distribution of oncogenic mutations and the parameter sensitivity are closely related. Our analysis clearly shows that mutations observed in tumor samples tend to be located in specific protein functional domains corresponding to the sensitive parameters of the bifurcation point.

Molecular Dynamics Simulation and ΔΔG Calculation. To dissect the mechanism underlying the correlation between oncogenic mutation distribution and parameter sensitivity, we conducted molecular dynamics simulations to compute protein–protein interaction kinetics. We aimed to answer two questions. How do cancer mutations cause alterations in the parameter sensitivities? How is this effect coordinated with shifts in the bifurcation point?

The Gibbs free energy change accompanying a protein–protein interaction can be represented by its equilibrium constant K_D, which can be linked to the kinetic parameters in the dynamic model [based on $\Delta G = RTln(K_D)$]. If a mutation causes a change in the free energy change of a protein–protein interaction, then the equilibrium constant K_D changes accordingly. Therefore, a logic chain connecting oncogenic mutations and parameter sensitivity can be established by mutation-induced change of free energy change in the protein–protein interaction. We propose that mutation-induced changes in free energy change ($\Delta\Delta G$) are one of the major causes of parameter sensitivity perturbations. These perturbations may cause a right shift of the bifurcation point in Fig. 2, which predisposes the cell to a nonapoptotic state.

To obtain the value of $\Delta\Delta G$ between wild-type and mutant protein systems, we built eight pairs of wild type–protein–protein interaction models (heterodimers in Fig. 1) based on the structural information for the corresponding proteins. Using wild-type models, we constructed single-mutation models according to the collected cancer-related mutations in corresponding functional domains. We also mutated each structure according to missense SNPs involved in the corresponding functional domain as controls. Therefore, we built 26 cancer-related mutations, 16 SNPs, and 8 wild-type complexes (*Supporting Information*). The free energy calculations were achieved using molecular dynamics simulation and molecular mechanics/generalized Born surface area (MM/GBSA) methods (see *Supporting Information* for details). We did not perform calculations of the entropy contribution to binding due to resource limitation; therefore, strictly speaking, our result is the binding energy of the protein complex rather than the Gibbs free energy change (Table S5). However, this simplification is not a limitation because our goal is to obtain the binding energy change between wild-type proteins and those

with single point mutations, which are very similar in structure. In most cases, the entropy difference can be ignored.

The ΔΔG calculation results for matched mutant/SNP–wild type are displayed in Fig. 5*A*, *Right*. In view of the parameter sensitivity of the bifurcation point (Fig. 5*A*, *Left*), the eight interactions were classified into three groups: sensitive, insensitive, and most insensitive (see different color regions in the Fig. 5*A*, *Right*). Mutations and SNPs involved in the same interaction are aligned in the same line.

To identify the oncogenic role of each mutation, we classified all mutations and SNPs into three categories designated as Right, Wrong, and Ordinary according to the mutational effect on the consistency between binding energy change and parameter perturbation direction, which are colored green, red, and blue, respectively (Fig. 5*A*, *Right*). The Right mutation is a mutation that produces a significant binding energy change, perturbs (increase or decrease) a parameter, and subsequently induces a right shift in the bifurcation point. We designate these mutations as Right because the mutation shows an oncogenic function by shifting the bifurcation point to a higher death threshold, consistent with our theoretical prediction. The Wrong mutation also produces a significant binding energy change and perturbs a parameter, but it induces a left shift in the bifurcation point. The Ordinary mutation does not produce a significant binding energy change and has no effect on the bifurcation point.

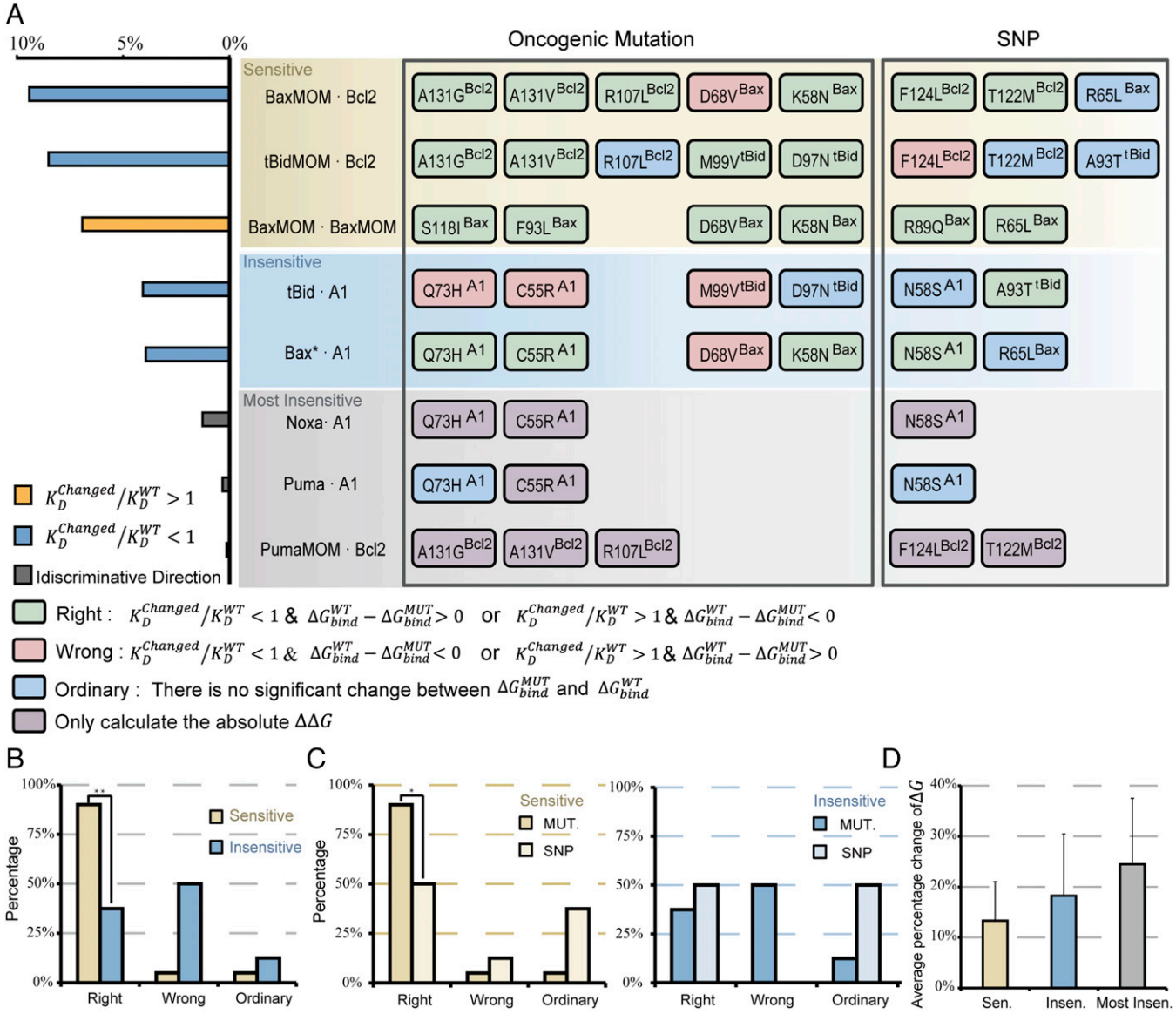

Fig. 5. Analysis of matched mutant/SNP and wild-type protein systems with respect to parameter sensitivity. (*A*) ΔΔG calculation result for matched mutant/SNP and wild-type protein systems with respect to parameter sensitivity. Mutations and SNPs involved in the same interaction are aligned in the same line. (*Left*) the percentage change of bifurcation point to the higher MOMP threshold in response to 10% K_D change. K_D, the equilibrium constant, is represented by the dissociation constant k_{off} for a certain interaction reaction (*Supporting Information*), whose value is directly extracted from the parameter sensitivity analysis (Fig. 3*A*). Colors of rectangles indicate the consistencies between parameter sensitivity analysis and calculation. (*B*) Comparison of Right, Wrong, and Ordinary distributions between sensitive and insensitive clusters. $^{**}P < 0.01$. *P* values were calculated using Fisher's test for odds ratios. See *Supporting Information* for counting rules and odds ratio calculation. (*C*) Comparison of Right, Wrong, and Ordinary distributions between sensitive group and SNP, and between insensitive group and SNP. $^{*}P < 0.05$. (*D*) Average relative change for nonordinary mutations in three sensitivity groups. The relative change refers to the percentage change for a matched mutant–wild type to the corresponding wild type. Insen., insensitive; Most Insen., most insensitive; Sen., sensitive. Error bars indicate ± SEM.

Parameter sensitivity analysis of the bifurcation point identifies two types of parameter perturbation that can induce a right shift of the bifurcation point: those that increase K_D ($K_D^{Changed}/K_D^{WT} > 1$, orange bar in Fig. 5*A*, *Left*), and those that decrease K_D ($K_D^{Changed}/K_D^{WT} < 1$, blue bar in Fig. 5*A*, *Left*). Therefore, based on $\Delta G = RTln(K_D)$, in cases of increase K_D, a Right mutation should satisfy $\Delta G_{bind}^{WT} - \Delta G_{bind}^{MUT} < 0$; otherwise it is a "Wrong" mutation. In cases of decrease K_D, a Right mutation should satisfy $\Delta G_{bind}^{WT} - \Delta G_{bind}^{MUT} > 0$, otherwise it is a Wrong mutation. For mutations involved in the most insensitive group, we only calculated the absolute value of ΔΔG owing to the undefinable sensitivity direction (Table S6).

Fig. 5*A* shows that the Right, Wrong, and Ordinary mutations/SNPs are not evenly distributed in different sensitivity groups. Statistical analyses of the Right, Wrong, and Ordinary mutation distributions of the first two sensitivity groups are shown in Fig. 5 *B* and *C*. Of 20 total mutations in the sensitive interactions, we found that 90% were Right mutations (Fig. 5*B*), which was significantly higher than that in insensitive interactions (37.5%) ($P < 0.01$, Fisher's test). Fig. 5*C*, *Left* shows that the Right mutations in sensitive interactions (90%) were greater than those in SNPs (40%) ($P < 0.05$, Fisher's test). This tendency was not observed in the insensitive group (Fig. 5*C*, *Right*). These results suggest that mutations in sensitive domains have high enrichment values and strong oncogenic function, whereas mutations in insensitive domains behave more like harmless SNPs.

To explore the mutational influence on wild-type binding energy in different sensitivity groups, we calculated the average relative change of binding energy (ΔΔG) for each nonordinary mutation in three sensitivity groups (Fig. 5*D*). The results showed a clearly increasing tendency of binding energy change from sensitive to most insensitive class. This suggests a distinct selection threshold for mutations in domains with different sensitivity. Sensitive parameters provide key regulatory positions in the regulatory network; a slight perturbation caused by a mutation will lead to qualitative changes in network behavior. Therefore, if we assume that each gene in the cell mutates more or less randomly (40), mutations occurring in sensitive domains tend to be selected out and reserved more easily than those in nonsensitive domains during the process of tumor evolution.

It is consistent with the experimental results that most of the involved mutations in sensitive interaction domains have high oncogenic potential. Some mutation sites in sensitive domains, including Bax, D68, and Bcl2 R107, are highly conserved and directly engaged in interactions with other Bcl2 family proteins (41). This suggests that severe disorders may arise in pathway function owing to variations in these sites. For example, Bax lacking the IGDE sequence (66–69 aa, including D68) failed to promote apoptosis in mammalian cells (42). Other work showed that Bax D68R could not dimerize with wild-type Bax in vitro, which is consistent with a previous computational simulation and our calculation for Bax D68V (43). These experimental results support our observation that mutations show their oncogenic function by affecting important protein interactions and thereby disrupting biological processes.

To show the mechanism of mutation-induced alterations in the binding energy, we used wild-type and mutant type D68V Bax dimer as an example for structural analysis. Previous research suggested that D68 and R109 tightly associate in the Bax dimer, and experiments demonstrated that the dimer cannot form with a mutation in either residue (43). Our computational analysis confirmed this result. In wild-type Bax dimer, D68 interacted with R109 by hydrogen bonding with strong electrostatic attraction, whereas this interaction disappeared when the negative charged amino acid aspartic acid was mutated to a hydrophobic amino acid valine (Fig. 6). As a result, the binding energy of Bax D68V dimer increased from wild-type −191 kcal/mol to −154 kcal/mol according to our calculation. The mutation Bax D68V dramatically altered the binding energy of Bax dimer toward the oncogenetic direction. Other structures of protein complexes with mutations highlighted were shown in Fig. S2.

Our calculation of the binding energy change between wild-type and mutant protein interactions provides some insight into the two questions we asked at the beginning of this section. The molecular mechanism responsible for the oncogenic effect of mutations lies in the changed binding kinetics of protein interactions (reflected by ΔΔG), and a consequent right shift of the bifurcation location. By exploring the underlying molecular mechanism, these results further support our hypothesis that interactions corresponding to the sensitive parameters have a crucial role in tumorigenesis, and mutations involved in sensitive interactions are most likely oncogenic.

Discussion

We successfully investigated the causal mechanism underlying the correlation between cancer mutation pattern of protein functional domains and parameter sensitivities of the system bifurcation by performing nonlinear dynamics and molecular-level analyses. We first conducted bifurcation analysis and parameter sensitivity analysis of the mitochondrial apoptotic pathway using a previously established method (15). Then, we separated functional and nonfunctional protein domains and mapped oncogenic mutations to the corresponding domains using structure information and established a correlation between parameter sensitivity of the bifurcation point and oncogenic mutation enrichment of functional domains. We further systematically studied the molecular mechanism underlying this correlation by evaluating the mutational effect on protein interaction kinetics using molecular dynamic simulation. We found that the binding energy changes induced by mutations are major determinants of parameter changes in the regulatory network model; combining the bifurcation point change direction due to parameter perturbation and the binding energy change direction due to mutation disturbance, we identified the oncogenic role of each mutation and found that mutations involved in sensitive interactions (corresponding to sensitive parameters of the bifurcation point) are most likely oncogenic. Finally, a clear vision of mutation-induced oncogenesis emerged after these analyses. The location of the

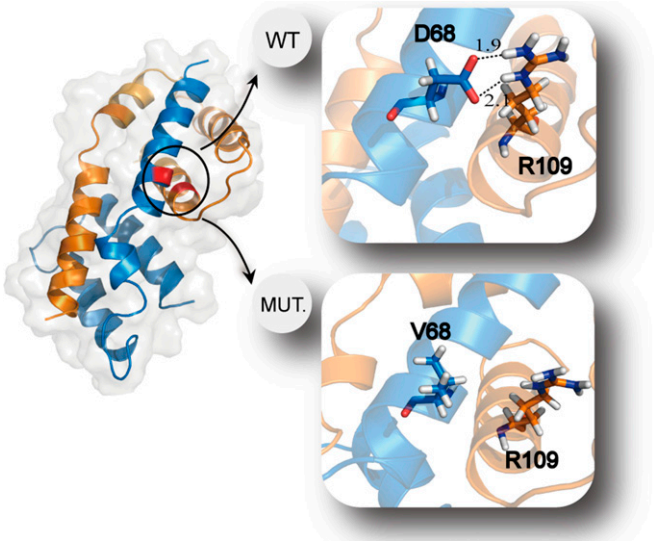

Fig. 6. Comparison of wild-type and mutant Bax dimer. The structures of wild-type and mutant Bax dimer were adopted by the structures with minimal binding energies in the duration of the molecular dynamic simulations, respectively. Dashed lines in the wild-type dimer structure indicate two hydrogen bonds with strong electrostatic attraction. There is no such interaction in the mutant dimer structure.

saddle-node bifurcation point represents a MOMP threshold; if this threshold is exceeded, the system switches on apoptosis. Oncogenic mutations may increase this threshold by introducing significant changes in binding kinetics between key regulators. Consequently, the death switch is averted and cells can evade apoptosis. These conditions may enable oncogenesis.

The correlation between domain mutation enrichment spectrum and parameter sensitivity spectrum of the bifurcation point suggests that bifurcation point perturbation is a good measure to predict causal genes and mutations in cancer. Stites et al. (14) proposed a protein-level, perturbation-based analysis of unregulated Ras activation associated with cancer and successfully explained the correlation between Ras mutation properties and the known pathological mechanisms of Ras signaling activation. In our opinion, the selection of different dynamic features should not be considered as an inconsistency; the specific biological function to be embodied should be taken into account. For apoptosis, G1/S transition or any other checkpoint-like processes, such as epithelial-to-mesenchymal transition, induce bifurcation behaviors reflecting the qualitative change of a system. This is a good measure for describing the switch-like cell fate decision from a dynamic point of view. The steady-state level of certain protein species (reflecting protein concentration) is more precise for evaluating signal transduction pathways that require proper concentrations of active kinases for activation (44). Considering these aspects, our analysis also can be applied to any apoptotic response pathways that share similar interaction topology and key regulators, with a bifurcation behavior as the pathway functional property.

The parameters in network analysis include binding/unbinding kinetic rates. Therefore, binding energy, a reflection of the equilibrium constant K_D, is not a direct indicator of network parameters. In this work, we assumed that the mutation effect on K_D is due primarily to the change of k_{off} (Fig. 5*A*, *Left*), considering that k_{on} is described based on diffusion rules and long-range force, which will not be significantly influenced by single mutation, whereas k_{off} is determined primarily by short-range interactions (ionic interactions, hydrogen bonds, and hydrophobic interaction) and is more likely to change due to amino acid variation (45). Our parameter sensitivity analysis also shows that even if the mutation has a significant effect on k_{on} under certain conditions it also would not bring discordance to the original results (*Supporting Information*). It will be more precise if we can specify the mechanisms of kinetic parameter change. Tiwary et al. (46) recently developed a method to calculate k_{off} of the interaction between a protein and its small molecule ligand. This method is based on metadynamics, which samples as many configurations as possible to rebuild the different binding phases at a large timescale. However, this method is not applicable for protein complex simulations with large sample space, and the accuracy is limited. Therefore, the method of calculating kinetic rates of protein–protein interactions by molecular dynamics simulation is at a very early stage. We hope this method will be fully developed in the future to further facilitate investigations such as the present study.

Our study selected a subset of parameters that represent specific protein interactions, including binding and membrane translocation, for analysis. The structural information of those selected protein interactions has been reported; therefore, we accurately mapped mutations to interaction domains and established the correspondence between mutations and model parameters. Further calculations also depended on structural information for the protein interactions. Some important factors were excluded from this analysis because sufficient information on the molecular mechanisms and interaction structures was not currently available. Nonexon mutations (47), transcription factor mutations (48), and proteasome mutations (49), which often affect protein expression levels and protein degradation processes and play important roles in cancer development, were out of the scope of our study, whereas we find some consistency between sensitivity of these kind of parameters and corresponding oncogenetic aberrations (*Supporting Information*). An analysis including those factors could provide a more complete picture of oncogenesis.

Materials and Methods

Equations for the Mitochondrial Apoptotic Network. We compiled a set of ODEs (*Supporting Information*) to model the mitochondrial apoptotic network induced by extrinsic death signals.

Cancer Mutation, SNP, and Protein Structure Database. All mutations in our analysis were obtained from COSMIC and literature. The missense SNPs were obtained from dbSNP. Some initial structure of wild-type protein complexes were obtained from Protein Data Bank (www.rcsb.org/pdb/home/home.do), and some were obtained by molecular replacement (*Supporting Information*).

Molecular Dynamics Simulation and MM/GBSA Method. All molecular dynamics simulations were performed using Amber software (version 11). Single trajectories were used to calculate the binding energy and residue energy decomposition using the MM/GBSA algorithm in AmberTools12 (*Supporting Information*).

ACKNOWLEDGMENTS. We thank J. Chen, L. H. Lai, F. J. Chen, X. M. Ma, D. Q. Yu, Y. S. Cao, H. Y. Fang, Z. W. Xie, X. Zhao, B. Shao, J. Y. Xi, H. L. Wang, and F. T. Li for helpful discussions. This work was partially supported by National Natural Science Foundation of China Grants 11074009 and 81273436 and Chinese Ministry of Science and Technology Grants 2012AA02A702 and 2012AA020301.

1. Kandoth C, et al. (2013) Mutational landscape and significance across 12 major cancer types. *Nature* 502(7471):333–339.
2. Dahl F, et al. (2007) Multigene amplification and massively parallel sequencing for cancer mutation discovery. *Proc Natl Acad Sci USA* 104(22):9387–9392.
3. Alexandrov LB, et al.; Australian Pancreatic Cancer Genome Initiative; ICGC Breast Cancer Consortium; ICGC MMML-Seq Consortium; ICGC PedBrain (2013) Signatures of mutational processes in human cancer. *Nature* 500(7463):415–421.
4. Stratton MR, Campbell PJ, Futreal PA (2009) The cancer genome. *Nature* 458(7239): 719–724.
5. Jones S, et al. (2008) Core signaling pathways in human pancreatic cancers revealed by global genomic analyses. *Science* 321(5897):1801–1806.
6. Ding L, et al. (2008) Somatic mutations affect key pathways in lung adenocarcinoma. *Nature* 455(7216):1069–1075.
7. Cancer Genome Atlas Research Network (2008) Comprehensive genomic characterization defines human glioblastoma genes and core pathways. *Nature* 455(7216): 1061–1068.
8. Bild AH, Potti A, Nevins JR (2006) Linking oncogenic pathways with therapeutic opportunities. *Nat Rev Cancer* 6(9):735–741.
9. Pe'er D, Hacohen N (2011) Principles and strategies for developing network models in cancer. *Cell* 144(6):864–873.
10. Kreeger PK, Lauffenburger DA (2010) Cancer systems biology: A network modeling perspective. *Carcinogenesis* 31(1):2–8.
11. Ferrell JE, Jr, Tsai TY, Yang Q (2011) Modeling the cell cycle: Why do certain circuits oscillate? *Cell* 144(6):874–885.
12. Zhang XP, Liu F, Cheng Z, Wang W (2009) Cell fate decision mediated by p53 pulses. *Proc Natl Acad Sci USA* 106(30):12245–12250.
13. Ma W, Trusina A, El-Samad H, Lim WA, Tang C (2009) Defining network topologies that can achieve biochemical adaptation. *Cell* 138(4):760–773.
14. Stites EC, Trampont PC, Ma Z, Ravichandran KS (2007) Network analysis of oncogenic Ras activation in cancer. *Science* 318(5849):463–467.
15. Chen J, Yue H, Ouyang Q (2014) Correlation between oncogenic mutations and parameter sensitivity of the apoptosis pathway model. *PLOS Comput Biol* 10(1): e1003451.
16. Tait SW, Green DR (2010) Mitochondria and cell death: Outer membrane permeabilization and beyond. *Nat Rev Mol Cell Biol* 11(9):621–632.
17. Spencer SL, Sorger PK (2011) Measuring and modeling apoptosis in single cells. *Cell* 144(6):926–939.
18. Chipuk JE, Bouchier-Hayes L, Green DR (2006) Mitochondrial outer membrane permeabilization during apoptosis: The innocent bystander scenario. *Cell Death Differ* 13(8):1396–1402.
19. Llambi F, Green DR (2011) Apoptosis and oncogenesis: Give and take in the BCL-2 family. *Curr Opin Genet Dev* 21(1):12–20.
20. Youle RJ, Strasser A (2008) The BCL-2 protein family: Opposing activities that mediate cell death. *Nat Rev Mol Cell Biol* 9(1):47–59.
21. Li H, Zhu H, Xu CJ, Yuan J (1998) Cleavage of BID by caspase 8 mediates the mitochondrial damage in the Fas pathway of apoptosis. *Cell* 94(4):491–501.
22. Lovell JF, et al. (2008) Membrane binding by tBid initiates an ordered series of events culminating in membrane permeabilization by Bax. *Cell* 135(6):1074–1084.

23. Kim H, et al. (2009) Stepwise activation of BAX and BAK by tBID, BIM, and PUMA initiates mitochondrial apoptosis. *Mol Cell* 36(3):487–499.
24. Hsu Y-T, Wolter KG, Youle RJ (1997) Cytosol-to-membrane redistribution of Bax and Bcl-X(L) during apoptosis. *Proc Natl Acad Sci USA* 94(8):3668–3672.
25. Tan C, et al. (2006) Auto-activation of the apoptosis protein Bax increases mitochondrial membrane permeability and is inhibited by Bcl-2. *J Biol Chem* 281(21): 14764–14775.
26. Happo L, Strasser A, Cory S (2012) BH3-only proteins in apoptosis at a glance. *J Cell Sci* 125(Pt 5):1081–1087.
27. Chen C, et al. (2007) Modeling of the role of a Bax-activation switch in the mitochondrial apoptosis decision. *Biophys J* 92(12):4304–4315.
28. Leber B, Lin J, Andrews DW (2007) Embedded together: The life and death consequences of interaction of the Bcl-2 family with membranes. *Apoptosis* 12(5):897–911.
29. Aldridge BB, Burke JM, Lauffenburger DA, Sorger PK (2006) Physicochemical modelling of cell signalling pathways. *Nat Cell Biol* 8(11):1195–1203.
30. Lu M, Jolly MK, Levine H, Onuchic JN, Ben-Jacob E (2013) MicroRNA-based regulation of epithelial-hybrid-mesenchymal fate determination. *Proc Natl Acad Sci USA* 110(45): 18144–18149.
31. Ferrell JE, Jr, et al. (2009) Simple, realistic models of complex biological processes: Positive feedback and bistability in a cell fate switch and a cell cycle oscillator. *FEBS Lett* 583(24):3999–4005.
32. Lee YS, Liu OZ, Hwang HS, Knollmann BC, Sobie EA (2013) Parameter sensitivity analysis of stochastic models provides insights into cardiac calcium sparks. *Biophys J* 104(5):1142–1150.
33. Yue H, et al. (2006) Insights into the behaviour of systems biology models from dynamic sensitivity and identifiability analysis: A case study of an NF-kappaB signalling pathway. *Mol Biosyst* 2(12):640–649.
34. Forbes SA, et al. (2015) COSMIC: Exploring the world's knowledge of somatic mutations in human cancer. *Nucleic Acids Res* 43(Database Issue):D805–D811.
35. Yamamoto H, Sawai H, Perucho M (1997) Frameshift somatic mutations in gastrointestinal cancer of the microsatellite mutator phenotype. *Cancer Res* 57(19):4420–4426.
36. Sherry ST, et al. (2001) dbSNP: The NCBI database of genetic variation. *Nucleic Acids Res* 29(1):308–311.
37. Billen LP, Shamas-Din A, Andrews DW (2008) Bid: A Bax-like BH3 protein. *Oncogene* 27(Suppl 1):S93–S104.
38. Schinzel A, et al. (2004) Conformational control of Bax localization and apoptotic activity by Pro168. *J Cell Biol* 164(7):1021–1032.
39. Gil J, Yamamoto H, Zapata JM, Reed JC, Perucho M (1999) Impairment of the proapoptotic activity of Bax by missense mutations found in gastrointestinal cancers. *Cancer Res* 59(9):2034–2037.
40. Vogelstein B, et al. (2013) Cancer genome landscapes. *Science* 339(6127):1546–1558.
41. Ku B, Liang C, Jung JU, Oh BH (2011) Evidence that inhibition of BAX activation by BCL-2 involves its tight and preferential interaction with the BH3 domain of BAX. *Cell Res* 21(4):627–641.
42. Zha H, et al. (1996) Structure-function comparisons of the proapoptotic protein Bax in yeast and mammalian cells. *Mol Cell Biol* 16(11):6494–6508.
43. Czabotar PE, et al. (2013) Bax crystal structures reveal how BH3 domains activate Bax and nucleate its oligomerization to induce apoptosis. *Cell* 152(3):519–531.
44. Dhillon AS, Hagan S, Rath O, Kolch W (2007) MAP kinase signalling pathways in cancer. *Oncogene* 26(22):3279–3290.
45. Schreiber G (2002) Kinetic studies of protein-protein interactions. *Curr Opin Struct Biol* 12(1):41–47.
46. Tiwary P, Limongelli V, Salvalaglio M, Parrinello M (2015) Kinetics of protein-ligand unbinding: Predicting pathways, rates, and rate-limiting steps. *Proc Natl Acad Sci USA* 112(5):E386–E391.
47. Fredriksson NJ, Ny L, Nilsson JA, Larsson E (2014) Systematic analysis of noncoding somatic mutations and gene expression alterations across 14 tumor types. *Nat Genet* 46(12):1258–1263.
48. O'Farrell TJ, Ghosh P, Dobashi N, Sasaki CY, Longo DL (2004) Comparison of the effect of mutant and wild-type p53 on global gene expression. *Cancer Res* 64(22): 8199–8207.
49. Tank EM, True HL (2009) Disease-associated mutant ubiquitin causes proteasomal impairment and enhances the toxicity of protein aggregates. *PLoS Genet* 5(2): e1000382.
50. Albeck JG, Burke JM, Spencer SL, Lauffenburger DA, Sorger PK (2008) Modeling a snap-action, variable-delay switch controlling extrinsic cell death. *PLoS Biol* 6(12): 2831–2852.
51. The 1000 Genomes Project Consortium (2010) A map of human genome variation from population-scale sequencing. *Nature* 467(7319):1061–1073.
52. Ikegaki N, Katsumata M, Minna J, Tsujimoto Y (1994) Expression of bcl-2 in small cell lung carcinoma cells. *Cancer Res* 54(1):6–8.
53. Monni O, et al. (1997) BCL2 overexpression associated with chromosomal amplification in diffuse large B-cell lymphoma. *Blood* 90(3):1168–1174.
54. Rampino N, et al. (1997) Somatic frameshift mutations in the BAX gene in colon cancers of the microsatellite mutator phenotype. *Science* 275(5302):967–969.
55. Gohlke H, Kiel C, Case DA (2003) Insights into protein-protein binding by binding free energy calculation and free energy decomposition for the Ras-Raf and Ras-RalGDS complexes. *J Mol Biol* 330(4):891–913.